sterdam, 1968); Ann. Rev. Nucl. Sci. 19 (1969); B. French, in *Proceedings of the Fourteenth International Conference on High Energy Physics, Vienna, Austria, 1968*, edited by J. Prentki and J. Steinberger (CERN, Geneva, Switzerland, 1968); B. Maglic, in *Proceedings of the Lund International Conference on Elementary Particles* (Ref. 12).

[43]S. Weinberg, in *Proceedings of the Fourteenth International Conference on High Energy Physics, Vienna, Austria, 1968* (Ref. 42); B. Renner, in *Proceedings of the Lund International Conference on Elementary Particles* (Ref. 12); S. Gasiorowicz and D. A. Geffen, Rev. Mod. Phys. 41, 531 (1969).

[44]Study of the Veneziano model for the $\sigma\pi^+\pi^-\pi^+\pi^-$ five-point amplitude suggested that the $A_1 \to \rho\pi$ decay is nonderivative, i.e., almost pure S-wave (J. Detlefsen, private communication). See also C. A. Savoy, Lett. Nuovo Cimento 2, 870 (1969) [later work on the 6π amplitude has not confirmed this result]; J. D. Dorren, V. Rittenberg, and H. R. Rubinstein, Nucl. Phys. B20, 663 (1970).

[45]D. J. Crennell *et al.*, Phys. Rev. Letters 24, 781 (1970).

[46]J. Ballam *et al.* [Phys. Rev. Letters 21, 934 (1968); Phys. Rev. D 1, 94 (1970)] favor a large D-wave component. In this analysis, a background amplitude having the angular dependence given by one-pion exchange has been subtracted.

[47]I. R. Kenyon *et al.*, Phys. Rev. Letters 23, 146 (1969); N. Armenise *et al.*, Lett. Nuovo Cimento 4, 199 (1970).

[48]D. Cohen *et al.*, University of Rochester report (unpublished).

[49]D. J. Crennell *et al.*, Phys. Rev. Letters 22, 1327 (1969); E. W. Andersen *et al.*, Phys. Rev. Letters 22, 1390 (1969); I. C. Berlinghieri *et al.*, Phys. Rev. Letters 23, 42 (1969); G. Caso *et al.*, Lett. Nuovo Cimento 3, 707 (1970).

[50]M. S. Robin *et al.*, Phys. Rev. Letters 24, 925 (1970); G. Garelick, *Experimental Meson Spectroscopy*, edited by C. Baltay and A. Rosenfeld (Columbia Univ. Press, New York, 1970).

[51]For example, at $s_1 = 1.15$ GeV^2 and $t_2 = -0.1$ GeV^2, we have $-0.07 > t_1 > -0.61$ GeV^2.

[52]F. Gilman *et al.*, Phys. Letters 31B, 387 (1970).

[53]H. Satz, Phys. Letters 32B, 380 (1970).

PHYSICAL REVIEW D VOLUME 5, NUMBER 9 1 MAY 1972

Survey of Inclusive Distributions in a Dual-Resonance Model*

G. H. Thomas
High-Energy Physics Division, Argonne National Laboratory, Argonne, Illinois 60439
(Received 29 December 1971)

From a numerical survey of the dual-resonance model (DRM), it is found that (i) scaling in the central region is approached much more slowly than in the fragmentation regions due partially to kinematics, and partially to the overlap of the two fragmentation regions; (ii) the triple-Regge limit of the model remains a good approximation over most of the fragmentation region, if it is multiplied by a simple modulating factor. The physical origin of such a factor deserves theoretical attention. (iii) If the exchange picture is taken seriously, one should expect wrong-signature-nonsense-zero dips in reactions such as $\pi^- + p \to \pi^0 + X$ for $x \gtrsim 0.2$. The phenomenological implications of the DRM are also discussed.

I. INTRODUCTION

In the past, dual-resonance models (DRM) have provided valuable insights into the structure of scattering amplitudes due to constraints of crossing symmetry, Regge behavior, and narrow-resonance behavior. These insights have been of both a theoretical and phenomenological character.[1] Most recently, attention has been centered on the qualitative application of dual models to inclusive reactions. DeTar, Kang, Tan, and Weis (DKTW)[2] have shown that this model contains many nice theoretical properties, such as limiting behavior in the central and fragmentation regions, triple-Regge asymptotic behavior, and a universal cutoff in transverse momentum of the form $e^{-4\alpha' p_\perp^2}$. A next step would be to study the quantitative applications to data.

Some work of this kind has been done already,[3] and raises many interesting questions concerning the shapes of inclusive distributions one might obtain in the model. To answer such questions, and to investigate further the phenomenological implications, we present in this paper a thorough numerical survey of inclusive shapes in the DRM.

Before proceeding to the numerical study, let us first briefly summarize inclusive reaction terminology.[4] The reaction

$$a + b \to c + X, \tag{1.1}$$

where X represents "anything," can be described in terms of the invariants

$$s=(P_a+P_b)^2,$$
$$M^2=(P_a+P_b-P_c)^2,$$
$$t=(P_b-P_c)^2, \tag{1.2}$$
$$u=(P_a-P_c)^2$$

(note that $s+t+u=M^2+m_a^2+m_b^2+m_c^2$), or equivalently in terms of s and the c.m. transverse ($P_\perp$) and longitudinal ($P_\parallel$) momenta of particle c. Closely related to the c.m. momentum variables are the variables κ and x:

$$\kappa=(P_\perp^2+m_c^2)^{1/2},$$
$$x=2P_\parallel/\sqrt{s}\ . \tag{1.3}$$

In the limit that the energy $\sqrt{s}$ becomes large, there are three physical regions of particular interest to us:

(i) *The fragmentation region* of b (a) corresponds to the momenta in the rest frame of particle b (a), $\vec{P}_c$, being small compared to the total energy. In terms of the above variables, this means $|t|$ ($|u|$) $\ll s$, or, equivalently, $\kappa \ll \sqrt{s}/2$ and $x>0$ ($x<0$).

(ii) *The central region* corresponds to the momenta, $\vec{P}_c$, in the c.m. frame being small compared to the total energy. In other words, $\kappa \ll \sqrt{s}/2$ and $|x|=|2P_\parallel/\sqrt{s}|\ll 1$. In this limit, $tu/s \approx \kappa^2$, and $|t|$, $|u|$, and s are large.

(iii) *The triple-Regge region* of b (a) is a special case of the fragmentation region corresponding to $s \gg M^2 \gg 1$ GeV^2.

We are interested in studying the *invariant cross section*

$$f(s,M^2,t)\equiv E_c\frac{d\sigma}{d^3P_c}(ab\to cX)\Big/\sigma_{ab}^{\text{tot}} \tag{1.4}$$

in these physical regions. (Note that we have included σ_{ab}^{tot} in the usual definition.)

We would like any model for the invariant cross section $f(s,M^2,t)$ to have certain general properties such as (1) crossing, (2) unitarity, (3) spin, (4) Regge behavior, (5) resonance behavior (in nonexotic channels). It is particularly hard to construct such a model if one attempts to make separate models for each of the exclusive processes represented by the implicit sum in (1.4) which, at high energies, ranges over a large number of reactions. Fortunately, Mueller[5] offers an easier approach by using a type of optical theorem to relate the invariant cross section to an appropriate discontinuity in M^2 of the forward three-to-three scattering amplitude

$$a+b+\bar{c}\to a+b+\bar{c}\ . \tag{1.5}$$

One is then left with a simpler task of finding a realistic three-particle scattering amplitude which has some of the above properties. At present, the best such model we know about is the DRM which has crossing, Regge, and resonance behavior, and a zero-resonance-width approximation to unitarity. It is thus a very interesting model with which to study the functional form of the invariant cross section, even though the inclusion of spin and a more exact treatment of unitarity may modify the results.

In Sec. II the essential features of the DRM are reviewed. In Sec. III for a specific DRM, formulas for the limiting distributions are given in a form which can be easily evaluated numerically. Then, in Sec. IV a numerical study of the invariant cross section is given. Finally, in Sec. V the implications of these results to physical processes are discussed, including a discussion of how limiting distributions are reached.

II. THE DUAL-RESONANCE MODEL

In this paper, we shall make use of certain features of the DRM, which we summarize here.[6] The DRM for (1.5) is a linear combination of generalized Veneziano six-point functions. Of the 60 diagrams corresponding to distinct permutations of the six external particles, only 18 give a nonzero contribution to the discontinuity in the missing mass. Physically, for a permutation to have a nonzero discontinuity, a, b, and $\bar{c}$ must couple to a resonance in the missing-mass variable and, hence, must be adjacent. In general, the remaining 18 permutations vanish in the central and fragmentation (including triple-Regge) regions, since the Pomeranchukon trajectory is not included in the model. Nevertheless, DKTW have argued that it is still possible to identify certain of the permutations with limiting behavior for $f(s,M^2,t)$. For example, in the fragmentation region of b, the four graphs in Fig. 1 have the leading behavior $s^{\alpha_v(0)}$, where $\alpha_v(0)$ is the trajectory exchanged in the $a\bar{a}$ channel. All other graphs in this region vanish exponentially in s. If the total cross section σ_{ab}^{tot} also is assumed to have the same leading behavior $s^{\alpha_v(0)}$, then the invariant cross section $f(s,M^2,t)$ will have a limiting distribution [i.e., $f(s,M^2,t)$ *scales*]. Similarly, there is scaling in the fragmentation region of a if the four graphs in Fig. 1 with $a\leftrightarrow b$ also have the leading behavior $s^{\alpha_v(0)}$. This follows if the leading trajectory in channel $b\bar{b}$ is the same as in $a\bar{a}$. If there is scaling in both fragmentation regions, DKTW show that there is necessarily scaling in the central region. Here, diagram I, the diagram common to both fragmentation regions, gives the only nonzero contribution to $f(s,M^2,t)$.

Our primary interest is to study the limiting behavior of f and, hence, there is no loss in generality to consider only the four graphs in Fig. 1. Numbering the external particles from 1 to 6 (e.g., starting with a and proceeding counterclockwise), each diagram is given by the standard form[7]

$$B_6 = \int_0^1 dx_1 \int_0^1 dx_2 \int_0^1 dy\, x_1^{-\alpha_{23}-1}(1-x_1)^{-\alpha_{12}-1}x_2^{-\alpha_{45}-1}(1-x_2)^{-\alpha_{56}-1}y^{-\alpha_{13}-1}(1-y)^{-\alpha_{25}-1}(1-x_1y)^{-\alpha_{35}+\alpha_{12}+\alpha_{25}}$$
$$\times(1-x_2y)^{-\alpha_{24}+\alpha_{56}+\alpha_{25}}(1-x_1x_2y)^{-\alpha_{25}-\alpha_{34}+\alpha_{35}+\alpha_{24}}, \tag{2.1}$$

where

$$\alpha_{ij} = \alpha_{ij}(s_{ij}) = \alpha_{ij}(0) + \alpha' s_{ij}, \qquad s_{ij} = (P_i + P_{i+1} + \cdots + P_j)^2 . \tag{2.2}$$

DKTW have computed the appropriate discontinuities of (2.1) for the various regions to find the invariant differential cross section $f(s, M^2, t)$. In the fragmentation region of b (t fixed as $s \to \infty$) each diagram contributes

$$f\left(\frac{M^2}{s}, t\right) = \left(\frac{M^2}{s}\right)^{\alpha_v}\left(-\frac{\alpha_{12}}{\alpha_{13}}\right)^{\alpha_{23}}\left(-\frac{\alpha_{56}}{\alpha_{13}}\right)^{\alpha_{45}}\int_0^\infty dy_1\int_0^\infty dy_2(1-y_1-y_2)^{\alpha_v}\,\theta(1-y_1-y_2)y_1^{-\alpha_{23}-1}y_2^{-\alpha_{45}-1}$$
$$\times\left(1-\frac{\alpha_{13}}{\alpha_{12}}y_1\right)^{\alpha_{23}+\alpha_{34}-\alpha_{24}}\left(1-\frac{\alpha_{13}}{\alpha_{56}}y_2\right)^{\alpha_{45}+\alpha_{34}-\alpha_{35}}\left(1-\frac{\alpha_{13}}{\alpha_{12}}y_1-\frac{\alpha_{13}}{\alpha_{56}}y_2\right)^{-\alpha_v-\alpha_{34}+\alpha_{35}+\alpha_{24}}, \tag{2.3}$$

where $\alpha_v = \alpha_{a\bar{a}}(0)$. The phases of the factors outside the integral are specified by $\alpha_{12} \to s + i\epsilon$ when "2" = "b" and $\alpha_{56} \to s - i\epsilon$ when "5" = "b". Otherwise, the factors are real. This choice of phases ensures that the correct discontinuities have been taken to obtain the (real and positive) invariant cross section. The invariant cross section for the central region is obtained from (2.3) by taking the limit $M^2/s \to 1$ and $|t| \to \infty$ with $(1 - M^2/s)t$ fixed. Note that in this limit, $-(1 - M^2/s)t = \kappa^2$.

Of secondary interest to us is the rate at which the DRM approaches its limiting behavior. To study this behavior, we make use of the duality of the model. As argued by DKTW, for sufficiently large missing mass squared, M^2, the discontinuity of (2.1) will be approximately the residue of the narrow resonance at $[M^2]$, the closest integer to M^2. Thus,

$$f = R_6 \Big/ \frac{\pi(s_{ab})^{\alpha_v}}{\Gamma(1+\alpha_v)} . \tag{2.4}$$

The residue R_6 is given by a product of beta functions $B(x, y)$ and a finite sum[8,9]:

$$R_6 = \pi B(-\alpha_{45}, -\alpha_{56})B(-\alpha_{12}, -\alpha_{23})\sum_{m=0}^{[M^2]}\sum_{n=0}^{m}\sum_{l=m-n}^{m}\frac{(1+\alpha_{34})_{[M^2]-m}}{([M^2]-m)!}\frac{(-z_{24})_{m-n}}{(m-n)!}\frac{(-z_{25})_{n+l-m}}{(n+l-m)!}$$
$$\times\frac{(-z_{35})_{m-l}}{(m-l)!}\frac{(-\alpha_{56})_n}{(-\alpha_{45}-\alpha_{56})_n}\frac{(-\alpha_{12})_l}{(-\alpha_{12}-\alpha_{23})_l}, \tag{2.5}$$

where $(x)_n \equiv \Gamma(x+n)/\Gamma(x)$, and where

$$\begin{aligned} z_{24} &= -\alpha_{24} + \alpha_{34} + \alpha_{23}, \\ z_{25} &= -\alpha_{25} + \alpha_{35} + \alpha_{24} - \alpha_{34}, \\ z_{35} &= -\alpha_{35} + \alpha_{45} + \alpha_{34} . \end{aligned} \tag{2.6}$$

The sum (2.5), which contains

$$\tfrac{1}{6}([M^2]+1)([M^2]+2)([M^2]+3)$$

terms, provides a convenient method of evaluating numerically the invariant cross section $f(s, M^2, t)$ at finite s, as long as the number of terms in the sum is not too large. When $[M^2]$ becomes large, (2.4) approaches the limiting form (2.3).

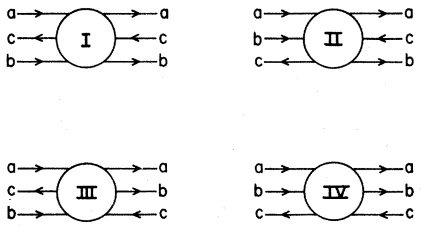

FIG. 1. The four dual-resonance diagrams which contribute in the fragmentation region of b. In the central region, only diagram I contributes.

III. THE LIMITING DISTRIBUTIONS

We start by evaluating the limiting distributions (2.3). The following simplifying assumptions are made:

(i) $\alpha_{a\bar{a}}(0)=\alpha_{b\bar{b}}(0)=\alpha_v$. As discussed above, this choice is necessary in order to obtain scaling in both the central and fragmentation regions. We also take $\alpha_v=1$, a choice which makes the computations easier.

(ii) $\alpha_{24}(t_{24})=\alpha_{35}(t_{35})=0$. Note that these numbers are of the type $\alpha_{a\bar{a}c}(m_c^2)=\alpha_{a\bar{a}c}(0)+\alpha' m_c^2$. To set this number to zero is equivalent to assuming particle c lies on the internal trajectory $\alpha_{a\bar{a}c}$.

As shown by DKTW, the invariant cross section is not sensitive to the numerical value of α_v, α_{24}, or α_{35}. Physically, this is because the discontinuity is (approximately) equivalent to the residue of the pole in M^2 of the six-point amplitude. The variables $t_{a\bar{a}}$, $t_{b\bar{b}}$, t_{24}, and t_{35} (such as $t_{a\bar{a}c}$, etc.) are all dual to M^2 and, hence, the residue, which can have no poles in these variables, is only weakly dependent on their exact values.

With these assumptions, the invariant cross section $f(s, M^2, t)$ is

$$f\left(\frac{M^2}{s}, t\right)=\frac{M^2}{s}\left[g_{\mathrm{I}}+g_{\mathrm{II}}e^{-i\pi\alpha}+g_{\mathrm{III}}e^{+i\pi\alpha}+g_{\mathrm{IV}}\right], \tag{3.1}$$

where the reality of f is assured by $g_{\mathrm{II}}=g_{\mathrm{III}}$. In (3.1), α is defined by

$$\alpha\equiv\alpha(t)\equiv\alpha_{a\bar{a}}(t_{a\bar{a}}), \tag{3.2}$$

and the g_i have the form

$$g_i\left(\frac{M^2}{s}, t\right)=|A_iB_i|^{-\alpha}\int_0^\infty dy_1\int_0^\infty dy_2(1-y_1-y_2)\,\theta(1-y_1-y_2)(y_1y_2)^{-1-\alpha}[(1-A_iy_1)(1-B_iy_2)]^{\alpha+\beta_i}$$
$$\times(1-A_iy_1-B_iy_2)^{-1-\beta_i}. \tag{3.3}$$

For g_{I}, $A_{\mathrm{I}}=B_{\mathrm{I}}=(x-1)/x$; for $g_{\mathrm{II}}=g_{\mathrm{III}}$, $A_{\mathrm{II}}=1-x$ and $B_{\mathrm{II}}=(x-1)/x$; and for g_{IV}, $A_{\mathrm{IV}}=B_{\mathrm{IV}}=1-x$. Here x is $1-M^2/s$, a good approximation when $s\gg\kappa^2/x^2$.

We now transform (3.3) into a form which can be conveniently evaluated numerically. With the change of variables

$$w_1=\frac{\{1+[(1-A)(1-B)]^{1/2}\}^2}{|AB|}\,\frac{Ay_1By_2}{(1-Ay_1)(1-By_2)},$$
$$w_2=\frac{1-A}{|A|}\,\frac{Ay_1}{1-Ay_1}, \tag{3.4}$$

Eq. (3.3) reduces to a form in which the w_2 integration can be done analytically. Performing this integration and making use of the connection between A, B, and $M^2/s=1-x$, we transform Eq. (3.3) into[10]

$$g_i(x,t)=\left(\frac{1-x}{1+x}\right)^{-2\alpha(t)}\times\int_0^1 dw\,w^{-1-\alpha(t)}\left[1-\left(\frac{1-x}{1+x}\right)^2w\right]^{\gamma_i}G_i(w). \tag{3.5}$$

Here,

$$G_i(w)=\ln\frac{w_{2i}^{(+)}}{w_{2i}^{(-)}}+\frac{1}{A_i}\ln\left|\frac{(1-A_i)/A_i+w_{2i}^{(-)}}{(1-A_i)/A_i+w_{2i}^{(+)}}\right|$$
$$+\frac{1}{B_i}\ln\left|\frac{(1-B_i)/B_i+w_{2i}^{(-)}}{(1-B_i)/B_i+w_{2i}^{(+)}}\right|. \tag{3.6}$$

The parameters γ_i, which are not dependent upon the invariants s, M^2, or t, have the values

$$\gamma_i=-2,\ \alpha_{b\bar{c}}(0)+\alpha_{bc}(0)+\alpha'(2m_b^2+2m_c^2),\ -1-\alpha_{c\bar{c}}(0) \tag{3.7}$$

for $i=$ I, II, and IV (recall $\gamma_{\mathrm{III}}=\gamma_{\mathrm{II}}$). Finally, the functions $w_{2i}^{(\pm)}$ are, for each diagram,

$$w_{2\mathrm{I}}^{(\pm)}=\frac{1}{2}\left(1+\frac{1-x}{1+x}w\pm\left\{(1-w)\left[1-\left(\frac{1-x}{1+x}\right)^2w\right]\right\}^{1/2}\right),$$
$$w_{2\mathrm{II}}^{(\pm)}=\frac{1}{2}\left\{1\pm(1-w)^{1/2}\Big/\left[1-\left(\frac{1-x}{1+x}\right)^2w\right]^{1/2}\right\}, \tag{3.8}$$
$$w_{2\mathrm{IV}}^{(\pm)}=\frac{1}{2}\left(1-\frac{1-x}{1+x}w\pm\left\{(1-w)\left[1-\left(\frac{1-x}{1+x}\right)^2w\right]\right\}^{1/2}\right).$$

Before evaluating (3.5) numerically, we check that the behavior in the triple-Regge limit ($x\to1$) and the central region ($x\to0$) agree with DKTW. In the first limit $x\to1$, the behavior of the integral is

determined by the behavior of $G_i(w)$ for $w \to 0$. For all four diagrams, as $w \to 0$,

$$G_i(w) \sim -\ln w + \frac{2x}{1-x}\ln x + 2\ln(1+x). \tag{3.9}$$

Thus, the invariant cross section f has the behavior

$$f \sim (1+e^{i\pi\alpha})(1+e^{-i\pi\alpha})\frac{(1-x)^{1-2\alpha}(1+x)^{2\alpha}}{\alpha^2} \times\left[1-\alpha\left(\frac{2x}{1-x}\ln x + 2\ln(1+x)\right)\right] \tag{3.10}$$

for $x \to 1$. The diagrams II, III, and IV serve the function of introducing the signature of the t-channel exchange. Note that for $x \neq 1$ there is a modulating factor which is unity at the particle pole $\alpha = 0$, and for $\alpha < 0$ is a decreasing function of x. As will be shown, a modification of Eq. (3.10) is a good approximation over a surprisingly wide range of x.

In the central region ($\alpha \to -\infty$ and $x \to 0$ with $-x\alpha \equiv \kappa^2$ fixed), the leading behavior is determined by values of the integrand near 1. In this limit, the g_i become [in units $\alpha' = 1$ (GeV/c)$^{-2}$]

$$g_{\mathrm{I}} \sim \frac{\sqrt{\pi}\, e^{-4\kappa^2}}{2^6\kappa^5}(4x)^{\gamma_{\mathrm{I}}+2}, \tag{3.11}$$

$$g_{\mathrm{II}} \sim \frac{\sqrt{\pi}}{2^6}\frac{e^{-4\kappa^2}}{\kappa^5}(4x)^{\gamma_{\mathrm{II}}+2}, \tag{3.12}$$

$$g_{\mathrm{IV}} \sim \frac{\sqrt{\pi}}{2}\frac{e^{-4\kappa^2}}{\kappa^3}(4x)^{\gamma_{\mathrm{IV}}+1}, \tag{3.13}$$

where γ_i are given by (3.7). Note that in order to obtain a limiting distribution for g_{I}, it is crucial that $\gamma_{\mathrm{I}} = -2$, which follows from the assumption $\alpha_{a\bar{a}}(0) = \alpha_{b\bar{b}}(0)$. Note also that the parameters γ_{II} and γ_{IV} determine how quickly the twisted graphs vanish, as the central region is approached.

IV. NUMERICAL ANALYSES OF THE DRM

In order to study the DRM thoroughly and economically, we must first make a judicious choice of variables. A convenient choice is

$$x = 1 - M^2/s, \qquad y = -x\alpha(t). \tag{4.1}$$

The variable x has a finite range $0 < x < 1$, and for practical application, y is similarly limited. Physically the variable y is $P_\perp{}^2$ when all the masses and intercepts are zero and the slopes are one.

We begin the study with diagram I which is given by Eq. (3.5). We define $R_{\mathrm{I}}(x, y)$ by

$$g_{\mathrm{I}}(x, y) = (1-x)^{+2y/x}\, e^{-2y}\left(\frac{x}{y}\right)^2 R_{\mathrm{I}}(x, y). \tag{4.2}$$

Evaluating $g_{\mathrm{I}}(x, y)$ numerically, our first result is that $R_{\mathrm{I}}(x, y)$ is approximately unity for $0.1 \lesssim x \lesssim 1$ (see Fig. 2). Except for $e^{-2y}R_{\mathrm{I}}(x, y)$, the factors in (4.2) are identically those of the triple-Regge limit. The surprising result is that over a large range in x and y where $g_{\mathrm{I}}(x, y)$ varies more than nine orders of magnitude, the triple-Regge form is modified only by a simple modulating factor e^{-2y}. Although we do not understand clearly why this should be the only modification, there seems to be experimental evidence for such a factor.[11] The physical origins of this factor deserve further study.

Our next result is that there may be a pronounced dip in the x distribution at $x = 0$ for fixed y (Fig. 2). In the zero-mass case, this can be understood by realizing that for fixed $P_\perp{}^2 (= y)$, α is smaller and closer to the first particle pole $\alpha = 0$ when x is near one than when x is near zero. It is

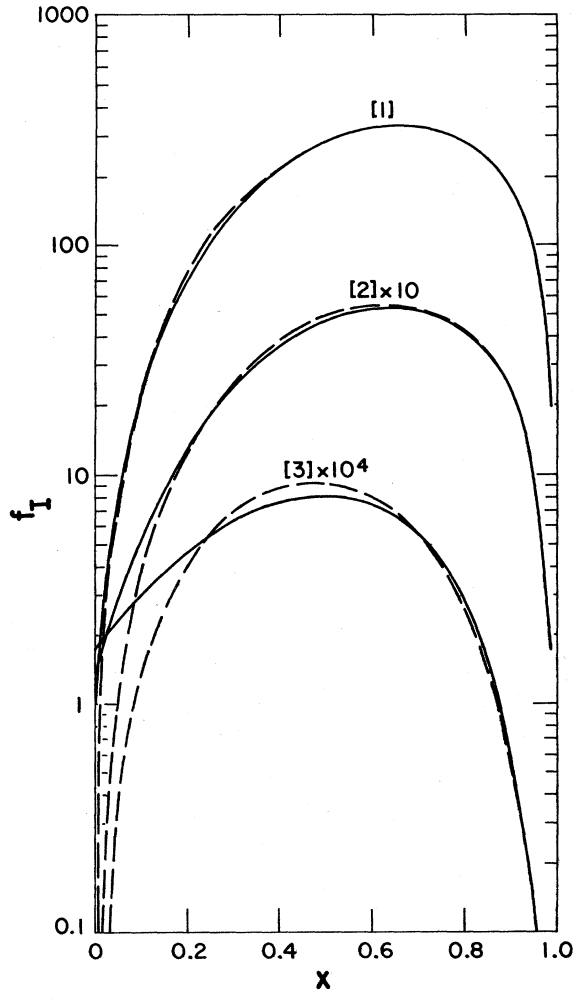

FIG. 2. The invariant cross section $(1-x)\,g_I(x, y)$ [solid curve, Eq. (3.5)] for $y = 0.02$ [1], 0.12 [2], and 1.02 [3]. The dashed curve is $(1-x)^{1-2\alpha(t)}\, e^{-2y}/\alpha(t)^2$.

clear from (4.2) that g_I should therefore exhibit more singular behavior for x near one than for x near zero. The factor $(1-x)^{-2\alpha}$ has the effect of shifting the maximum somewhat away from $x=1$. For other choices of external masses and intercepts, one may expect a similar behavior for fixed $P_\perp^2$ with the maximum of the x distribution occurring when t is nearest the first pole.

The strong effect of the first pole on the behavior of $g_I(x, y)$ is seen also in the y distributions for fixed x (Fig. 3). Note that as x increases, the curves become steeper at small y corresponding to $\alpha = -y/x$ moving closer to the pole.

A study of the "twisted" graphs reveals the presence of wrong-signature nonsense zeroes (WSNZ) for all $x>0$. These WSNZ show up as dips (assuming a positive-signature trajectory) for

$$\alpha(t) = -1, -3, -5, \ldots . \tag{4.3}$$

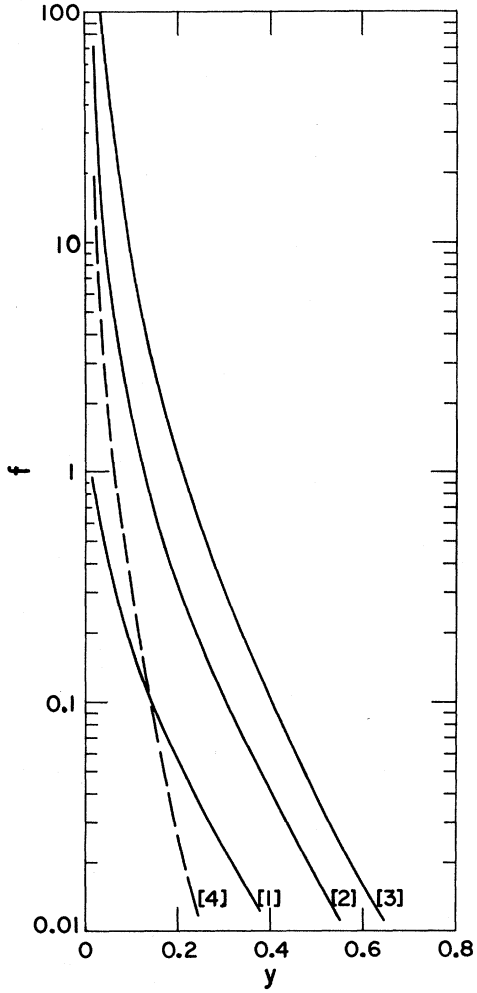

FIG. 3. The invariant cross section $(1-x)g_I(x, y)$ [Eq. (3.5)] for $x = 0.001$ [1], 0.2 [2], 0.7 [3], and 0.99 [4]. Curve [1] approximates the invariant cross section in the central region.

The magnitude of the effect depends upon the values of the parameters γ_{II} and γ_{IV}, which determine how rapidly the twisted graphs vanish in the central region [see Eqs. (3.12)–(3.13)]. Figure 4 shows for various choices of γ_{II} and γ_{IV} that there is noticeable structure in the invariant cross section at $x=0.1$. For $x \gtrsim 0.6$ and the choices of γ_{II} and γ_{IV} given in Fig. 4, the structure is approximately

$$f(x, y) \approx 4(1-x)g_I(x, y)\cos^2(\tfrac{1}{2}\pi\alpha), \tag{4.4}$$

with the approximation becoming exact as $x \to 1$. The approximation is based upon the numerical fact that in this region

$$g_I(x, y) > g_{II}(x, y), \quad g_{IV}(x, y) > 0.9\, g_I(x, y). \tag{4.5}$$

Equation (4.4) then follows from inserting (4.5) into (3.1).

The structure due to WSNZ shows up also in the x distributions (Fig. 5) for fixed y. Once again, we see oscillations which damp out to zero as $x \to 0$, but which are significant for $x \gtrsim 0.1$–0.2. We note that Bebel *et al.*[3] have found similar oscillations in the DRM, but the details of their calculation disagree with ours for small x. They obtain a considerably larger effect in this region, presumably

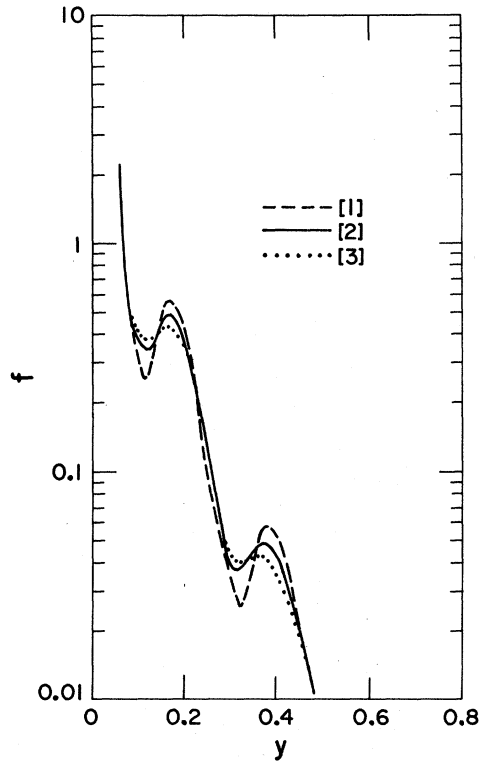

FIG. 4. The invariant cross section f [Eq. (3.1)], with $x = 0.1$ for various choices of the parameters γ_{II} and γ_{IV}: $\gamma_{II} = -1.0$, $\gamma_{IV} = -0.9$ [1]; $\gamma_{II} = 0.0$, $\gamma_{IV} = -0.5$ [2]; and $\gamma_{II} = 1.0$, $\gamma_{IV} = 0.0$ [3].

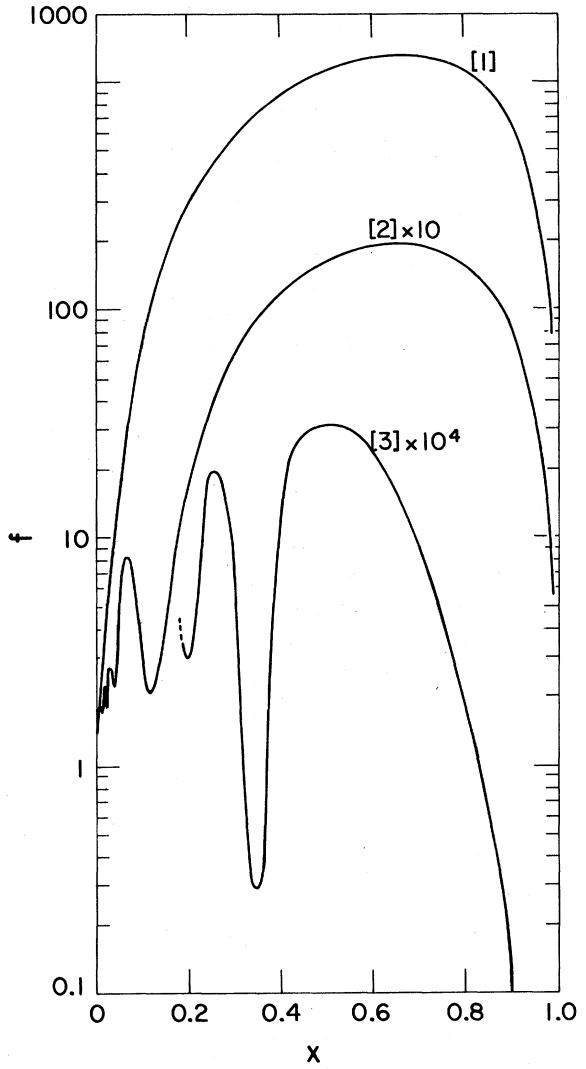

FIG. 5. The invariant cross section f [Eq. (3.1)], with $\gamma_{II} = 0.0$ and $\gamma_{IV} = -0.5$ for $y = 0.02$ [1], 0.12 [2], and 1.02 [3].

due to quite different choices for γ_{II} and γ_{IV}.

V. IMPLICATIONS FOR PHENOMENOLOGY

First we discuss the complications to the DRM which occur when one attempts to introduce physical trajectories. If the first particle on the trajectory α has spin J, the problem is (1) to avoid unphysical states for $\alpha < J$; (2) to ensure that, for $\alpha = J$, the residue has at least the behavior appropriate to a spin-J particle; and (3) to ensure that the amplitude has leading triple-Regge behavior, namely, $f \sim s^{2\alpha-1}$. One solution to this problem in the fragmentation region of b as $s \to \infty$ is to replace $\alpha(t)$ by $\alpha(t) - J$ in each of the dual amplitudes g_i given by (3.5), and then multiply the result by $(s/M^2)^{2J}$:

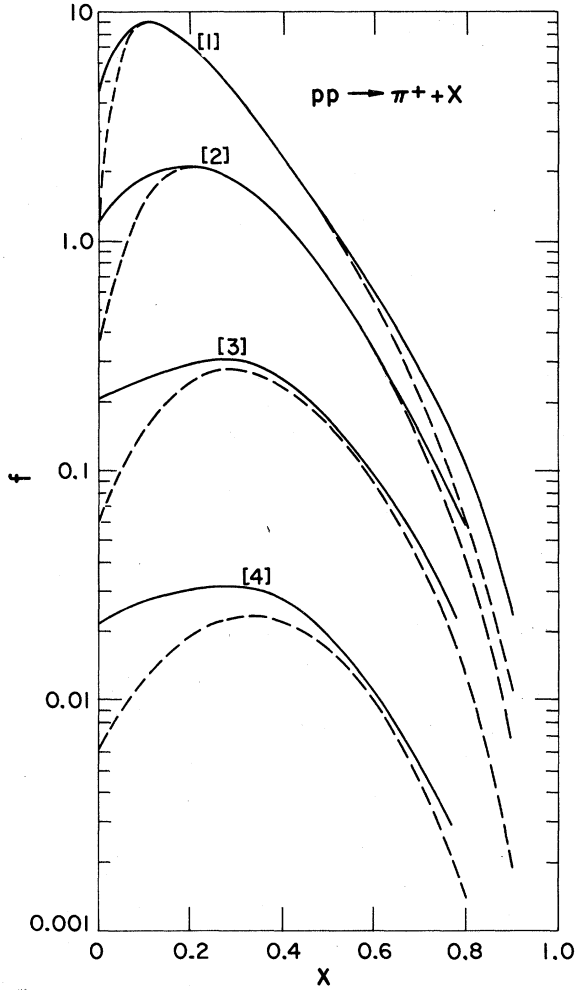

FIG. 6. The invariant cross section for $pp \to \pi^+ + X$ at 18 GeV/c assuming $N_\alpha - N_\gamma$ exchange in the t channel, for $P_\perp{}^2 = 0.0$ [1], 0.05 [2], 0.20 [3], and 0.50 [4]. The solid curve is computed using Eq. (2.5) at 18 GeV/c and is compared with the limiting distribution (dashed curve) $g_1(x, a - \frac{1}{2}) \times (1-x)^{1-1}$, given by Eq. (3.5). Equation (5.1) is used to define the model for this physical process.

$$g_i\left(\frac{M^2}{s}, \alpha(t)\right) \to \left(\frac{s}{M^2}\right)^{2J} g_i\left(\frac{M^2}{s}, \alpha(t) - J\right). \qquad (5.1)$$

Thus, the lowest spin on the parent trajectory is J, and the residue for $\alpha = J$ depends upon s^J, which is a polynomial of degree J in the cosine variable dual to t: the highest spin at the pole is J. In the triple-Regge limit, the factor $(M^2)^{2J}$ ensures that the leading behavior scales to $(s/M^2)^{2\alpha-1}$ for the invariant cross section. Of course, any polynomial factor of degree $2J$ would also give a solution. Moreover, a more precise approach to this problem might be to assume only that invariant amplitudes are given by dual functions. In such cases, still more complicated kinematic factors can result which depend upon s, M^2, and t.[12]

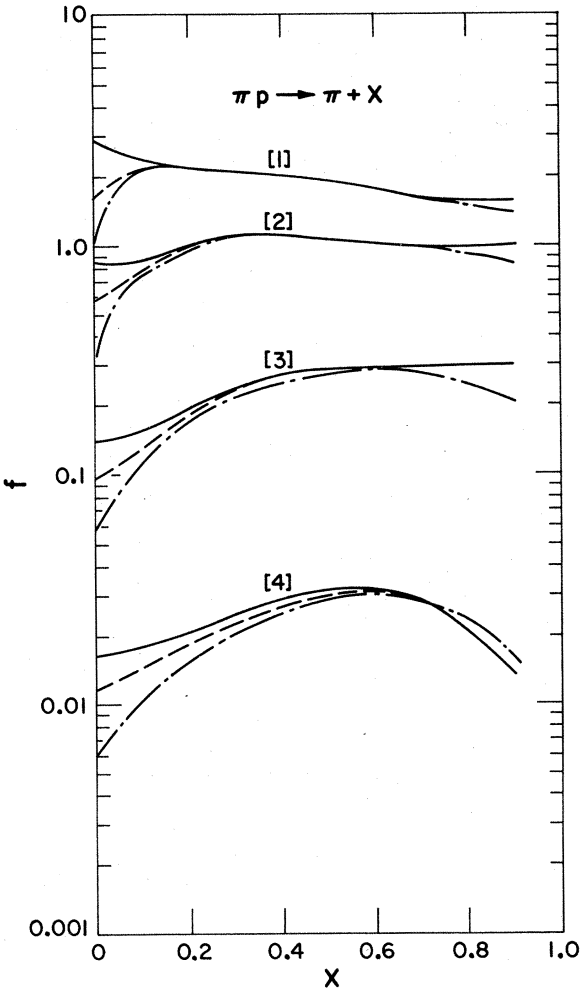

FIG. 7. The invariant cross section for $\pi p \rightarrow \pi + X$ at 18 GeV/c assuming $\rho - f$ exchange in the t channel for $P_\perp{}^2 = 0.0$ [1], 0.05 [2], 0.20 [3], and 0.50 [4]. The solid curve has $N_\alpha - N_\gamma$ exchange in the u channel, and the dashed curve has $\Delta_\delta - \Delta_\gamma$ exchange in the u channel. These curves are computed using (2.5) with (5.1) defining the model for this physical process. For comparison, the asymptotic distributions (dash-dot curves) are also given as in Fig. 6.

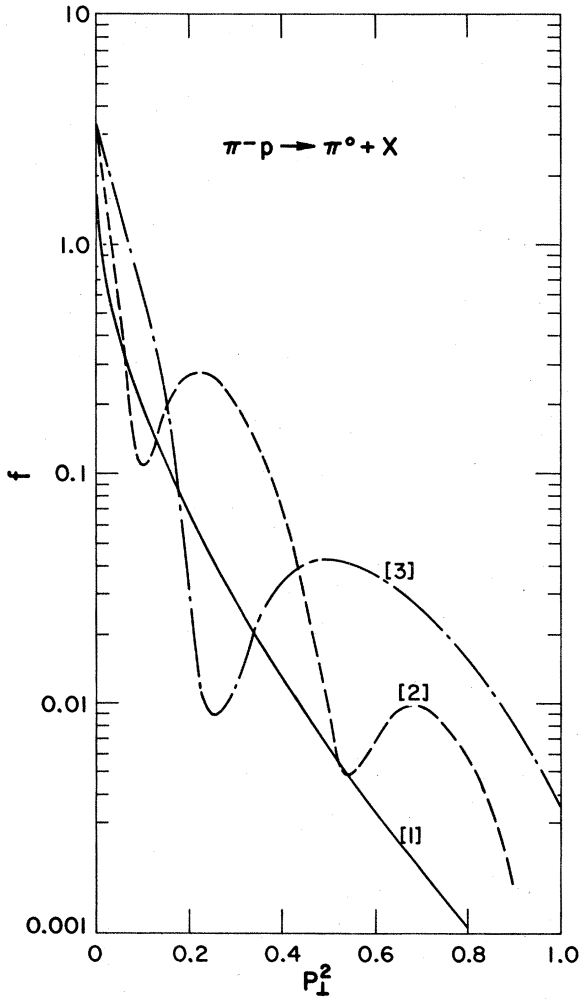

FIG. 8. The invariant cross section for $\pi^- p \rightarrow \pi^0 + X$ assuming ρ exchange for $x = 0.01$ [1], 0.2 [2], and 0.5 [3]. All four diagrams in Fig. 1 are included with (5.1) and (3.1) defining the model for this process. The parameters $\gamma_{II} = -0.2$ and $\gamma_{IV} = -0.5$ are chosen as representative values of (3.7).

The second point is that the predictions of the DRM at experimental energies will, in general, be slightly different from the limiting distributions described in the previous sections. A common way to present data is in terms of the c.m. transverse, $P_\perp$, and longitudinal $P_\parallel$ momenta or, equivalently, in terms of $P_\perp{}^2$ and

$$x = 2P_\parallel/\sqrt{s} \ . \tag{5.2}$$

In general, x is not equal to $1 - M^2/s$ unless

$$s \gg \kappa^2/x^2 \ . \tag{5.3}$$

For the limiting distributions in Sec. III, this condition was assumed to be satisfied in writing $x = 1 - M^2/s$. Note that in Fig. 6, the curve for finite s approaches the limiting distribution whenever condition (5.3) is satisfied, which occurs for $x \gtrsim 0.1$–0.2. Thus, we see that scaling in the central region is approached more slowly than in the fragmentation region.

A related point is that the u-channel exchange at finite energy has a strong effect around the central region (Fig. 7), but not in the b fragmentation region. This effect is similar to the effect induced by the s behavior of the model.

Our next observation is that the shapes of inclusive spectra depend sensitively on the trajectory intercepts and external masses (compare Figs. 6 and 7). To understand why this is so, it is sufficient to consider limiting distributions. When s is large [condition (5.3)], then

$$t \cong -\kappa^2/x + m_a^2(1-x) + m_c^2 . \quad (5.4)$$

As shown in the previous section, we expect the x distribution to have a maximum near where $\alpha(t)$ is closest to J, the nearest pole in the invariant cross section. This occurs when t reaches its maximum,

$$t_{\max} = m_a^2 + m_c^2 - 2\kappa m_a$$

for

$$x_{\max} = \kappa/m_a . \quad (5.5)$$

At $P_\perp^2 = 0$, for the process $pp \to \pi^+ X$, $x_{\max}$ is 0.15 and $t_{\max} = +0.6$; whereas, for $\pi p \to \pi X$, $x_{\max}$ is 1 and $t_{\max} = 0$. Thus, in the former reaction, the nucleon pole is near the physical region for small x producing a sharp maximum there. In the latter reaction, the ρ pole is most closely approached at $x = 1$ and, hence, the maximum is shifted.

It has been pointed out elsewhere[11] that the above result is more general than the DRM. In any model where the dynamics of the invariant cross section can be understood by means of t-channel Regge pole exchange, we expect that $f(s, M^2, t)$ will depend sensitively upon $\alpha(t)$ and, hence, upon the external masses and trajectory intercept.

The last point is that, as mentioned earlier, there can be pronounced WSNZ outside the triple-Regge region. For $\pi^- p \to \pi^0 + X$ (Fig. 8), the first dip occurs for $\alpha_\rho = 0$, corresponding to $t \cong -0.5$. It would be of tremendous theoretical interest to establish the presence or absence of such dips since, in principle, only one known trajectory contributes. The presence of such dips would be a strong confirmation of any simple Regge pole t-channel picture.

ACKNOWLEDGMENTS

I am indebted to Chan Hong-Mo, Paul Hoyer, and Richard Arnold for stimulating discussions at various stages of this work. In addition, it is a pleasure to thank Edmond L. Berger for his invaluable criticism of the manuscript.

---

*Work performed under the auspices of the U. S. Atomic Energy Commission.

[1]For a recent review of the phenomenological applications of crossing-symmetric (dual) models, see E. L. Berger, in *Phenomenology in Particle Physics 1971*, proceedings of the conference held at Caltech, 1971, edited by C. B. Chiu, G. C. Fox, and A. J. G. Hey (Caltech, Pasadena, 1971), p. 83.

[2]C. E. DeTar, K. Kang, C.-I Tan, J. H. Weis, Phys. Rev. D 4, 425 (1971). See also D. Gordon and G. Veneziano, *ibid.* 3, 2116 (1971); M. Virasoro, Phys. Rev. D 3, 2834 (1971).

[3]R. C. Arnold and S. Fenster, Argonne Report No. ANL/HEP 7122, 1971 (unpublished); D. Bebel, K. J. Biebl, D. Ebert, and H. J. Otto, Berlin University report, 1971 (unpublished); R. C. Brower and R. E. Waltz, Nuovo Cimento (to be published).

[4]See, e.g., E. L. Berger, *Proceedings of the Colloquium on Multiparticle Dynamics, University of Helsinki, 1971*, edited by E. Byckling, K. Kajantie, H. Satz, and J. Tuominiemi (University of Helsinki, 1971), p. 326.

[5]A. H. Mueller, Phys. Rev. D 2, 2963 (1970).

[6]The theoretical discussion in this section follows that of DKTW in Ref. 2.

[7]Chan Hong-Mo and Tsou Sheung Tsun, Phys. Letters 28B, 485 (1969).

[8]J. F. L. Hopkinson and E. Plahte, Phys. Letters 28B, 489 (1969).

[9]I thank Dr. P. Hoyer for pointing out to me this method of computing the discontinuity.

[10]For diagram II, one further change of variables was made to obtain the common factor $[(1-x)/(1+x)]^{-2\alpha(t)}$.

[11]Ph. Salin and G. H. Thomas, Nucl. Phys. (to be published).

[12]An example of this will appear shortly for the reaction $pp \to \pi^\pm + X$. See E. L. Berger, Ph. Salin, and G. H. Thomas, Phys. Letters (to be published).